École polytechnique de Louvain

Measurement of fingerpad deformation and force adjustment when performing vertical oscillations with hand-held objects

Author: **Hélène Nokerman**
Supervisors: **Philippe Lefèvre, Benoît Delhaye, Félicien Schiltz**
Reader: **André Mouraux**
Academic year 2019–2020
Master [120] in Biomedical Engineering

Acknowledgements

At first, I would like to express my gratitude to Prof. Philippe Lefèvre, who gave me the opportunity to address this interesting topic and to get a glimpse of what working in a research laboratory looks like, as well as for his guidance and advice throughout this project.

I would also like to greatly thank Benoît Delhaye and Félicien Schiltz for their help, support, availability and experience of which they made me take advantage throughout the different phases of the research over the year.

I would then like to thank Prof. André Mouraux who agreed to give some of his time to be part of the thesis jury as a reader.

I would finally like to extend my warmest thanks to my family and friends, for their unconditional support and encouragements not only during this project achievement but also throughout my studies. Some of them gave me a hand (*or at least fingers*) for the successful completion of this master thesis and I am very appreciative of that. This work would not have been possible without all of them.

Abstract

Object manipulations are part of the human daily life. They require the integration of various information by the central nervous system to enable the continuous adaptation of the force generated by the muscles to the desired task. One part of this required information is given by the tactile system with its mechanoreceptors innervating the fingertips. These receptors perceive the mechanical deformations appearing at the contact between the fingertips and the object and transmit this information to the central nervous system. Analysing these mechanical deformations can therefore be useful to understand how the continuous adaptation of the force takes place.

An experimentation, during which the contact area between the index fingertip of the subject and the object was imaged and the involved forces were recorded, was therefore performed: 12 subjects realised vertical oscillations with a fully counterbalanced object held in precision grip. The influence of the frictional conditions and the moisture skin level were also analysed.

Contents

1 Introduction **1**
1.1 General introduction . . . 1
1.2 Force control in precision grip . . . 1
1.3 Mechanical properties of the finger pad . . . 2
1.4 Finger pad deformations studies . . . 3
1.5 Aims of the project . . . 4

2 Material and methods **5**
2.1 Data collection . . . 5
2.1.1 Participants . . . 5
2.1.2 Apparatus and setup . . . 5
2.1.3 Experimental procedure . . . 8
2.2 Data analysis . . . 9
2.2.1 Data signals . . . 9
2.2.2 Fingerprint images . . . 12
2.3 Statistical analysis . . . 15

3 Results **16**
3.1 Coefficients of friction . . . 17
3.2 Moisture evolution . . . 19
3.3 Correlation between moisture and coefficients of friction . . . 21
3.4 Kinematics and dynamics . . . 22
3.4.1 Standard trial . . . 22
3.4.2 Grip force evolution . . . 23
3.4.3 Grip force modulation evolution . . . 26
3.4.4 Safety margin evolution . . . 27
3.5 Finger pad deformations . . . 29
3.5.1 Center of pressure position evolution . . . 29
3.5.2 Slips detection . . . 30
3.5.3 Surface strain rates analysis . . . 31

4 Conclusion **33**

5 References **34**

1 Introduction

1.1 General introduction

Dexterous grasping manipulations in precision grip, i.e. holding objects between the thumb and the index, are part of the human daily life. Although holding a pen, a key or even a needle seems quite simple at first glance, this type of execution requires to precisely coordinate forces, which are generated by several muscles and have to be adapted to the desired task, to the held object and to the surrounding environment. These manipulations therefore require the continuous integration of a considerable amount of sensory, proprioceptive and visual information by the central nervous system. [1]

Tactile sensory feedback is therefore of crucial importance when handling objects. It results from the encoding of information by numerous mechanoreceptors innervating the fingertips at the contact point with the object. On this basis, the central nervous system is able to assess physical properties of the object, among which are its shape, its surface roughness and its friction, which contribute to the proper force modulation. During manipulations, continuous complex mechanical interactions between the objects and the fingertips occur, which are what is encoded by the mechanoreceptors. Tactile feedback is therefore directly related to these mechanical interactions, which are still nowadays not fully understood. [2] [3]

Although more and more research is carried out on this subject, leading to some interesting results, potential for further exploration is still large. This master thesis therefore falls within this context.

1.2 Force control in precision grip

When manipulating an object in precision grip, the fingertip-object interaction forces can always be split into the normal (GF) and the tangential (LF) components at the contact surface. The first mentioned force is the one controlled and applied by the manipulator, while the second results from the gravitational and inertial forces of the object. Their respective representation is available on Figure 1A. [4]

To maintain an efficient grip, the applied grip force has always to be higher than the slip force, i.e. the minimal grip force to avoid the slipping of the object, which depends on the friction and the load force. There is therefore always a coupling between the grip and the load forces to ensure the proper handling of the object. This forces coupling is shown on Figure 1B. [4]

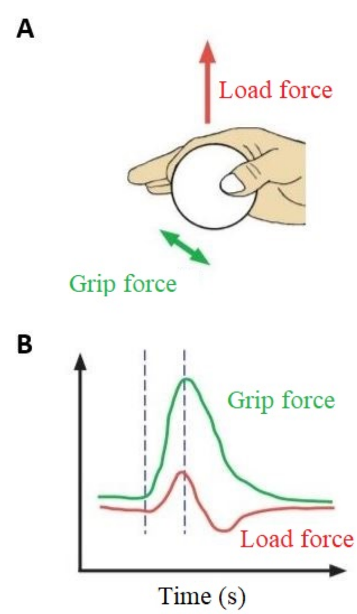

Figure 1: Force coordination. [4]

To ensure an adapted application of grip force to the desired task, the central nervous system has to collect and integrate information about the object as well as the surrounding environment. As aforementioned, this information is of tactile, visual and proprioceptive nature. Visual cues are particularly useful to prepare for the grasp of the object, by visually assessing the force to apply. It can also serve to apprehend the surrounding environment which could disrupt the handling in progress for example.
The proprioceptive information is responsible not only for sending information about the position and the movement of each part of the body to the central nervous system, but also to transmit to it information to maintain good posture and body balance.
The tactile information is encoded by the mechanoreceptors densely innervating the fingertip activated by the deformations occurring in the finger pad in contact with the object. It enables the assessment by the central nervous system of the mechanical properties of the object such as its friction or roughness. The influence of the cutaneous feedback for the proper grip force modulation when holding an object in precision grip has been the focus of numerous studies, which have all demonstrated its importance ([5], [6], [7], [8]).

As the load force also comprises an inertial component, the expected dynamics of the hand and the object has also to be taken into account in the coupling of the grip and load forces. This information can be obtained from the internal models. [3]

The force modulation during manipulations is therefore possible thanks to interaction of two different processes of control in parallel: the feedforward and the feedback controls. The first mentioned process is based on the internal models to predict change in the load force as well as the dynamics of the hand and the object whereas the second process relies on the sensory information (tactile, visual and proprioceptive) sent to the central nervous system. Both processes work in a complementary way during manipulations: the feedback control enables internal models predictions of the feedforward control to update whereas this latter compensates the delay of transmission between the receptors and the central nervous system of the sensory information. [3]

It is also interesting to note that with practice, some adaptation of the grip force to the performed task can occur so as to improve the efficiency of the movement. This is due to a modification in the internal models, which can be either temporary or permanent. If it is permanent, it is not called adaptation but learning. [4]

1.3 Mechanical properties of the finger pad

The mechanical deformations that occur when the fingertips come into contact with the object during handling depend in particular on the mechanical properties of the fingertips. It is therefore important to review them.

Firstly, when applying force on an object, the finger pad undergoes deformations that can be of considerable importance. For large deformations, a skin stiffening, which is non-linear, appear due to the progressive reorientation and loading of the rigid collagen fibers that were initially randomly coiled at rest. Moreover, due to the presence of epidermal ridges at the surface of the fingertips skin and mostly because the skin is stiffer along than across them, it can also undergo large shear and stretch deformations.
Another characteristic of the skin is that the moisture level of its upper layer has a big impact on

its mechanical properties: the higher its moisture level, the less brittle it becomes.
It is also interesting to note that under dynamic loading, the behaviour of the finger pad is visco-elastic, which means that it behaves elastically for low stimulation frequencies and viscously at higher frequencies. [3]

1.4 Finger pad deformations studies

The mechanical behaviour of the finger pad has been modelled as a homogeneously elastic sphere. Under this condition, when tangential loading is applied on it against a surface, specific deformations take place at the contact surface. Under low tangential loading, the periphery of the contact area between the finger pad and the surface starts to slip, in the direction of the loading, without extending to the central part of the contact area. If the tangential loading then increases, the slipping extends to the central stuck area, leading to the slipping of the whole contact. [3]

Although the finger pad cannot be considered as a homogeneous elastic sphere, the emergence of imaging techniques enabling the imaging of the fingertip-object surface, confirmed that the finger pad behaves as predicted, as depicted on Figure 2. From a terminological point of view, the slippage appearing at the periphery of the contact area is called partial slip or incipient slip, and when it extends to the central area previously stuck leading to the slip of the whole contact, it is called a full slip. [9]

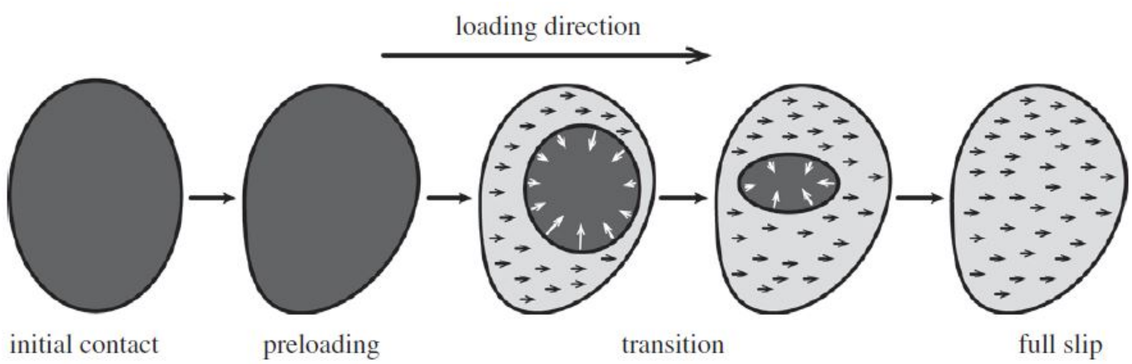

Figure 2: Steps from initial contact to full slip under loading. [9]

Since these imaging techniques have been introduced, several research have been carried out to study the mechanical behaviour of the finger pad. Here is a non-exhaustive list with their main findings.

In 2011, André et al. ([9]) conducted an experiment to analyse the influence of the skin moisture level on the transition from a fully sticking contact area to a fully slipping contact area between a surface and the fingertip. Based on the ratio between the slipping and the total area, it was found that the higher the humidity level, the smaller likelihood to slip. Moreover, when the skin exhibits a low moisture level, i.e. when the skin is dry, the nervous system tends to overcompensate by increasing the grip force.

In 2014, Delhaye et al. ([10]) investigated the skin deformation at the interface between the finger and a flat surface at the onset of tangential sliding movements, which vary in their directions (4 different directions were used) as well as in their tangential speeds. Different values of normal force were also tested. The obtained results highlighted the non-linear stiffening of the skin under high tangential load values due to the alignment of the collagen fibres initially at rest, resulting in a reduction of the contact area between the fingertip and the surface. Moreover, the finger pad deformation varied depending on the directions of the tangential sliding, in their shape as well as in their amplitude. The final conclusion of this article was that the central nervous system probably captures sensory information from these specific and reproducible deformations.

In 2016, Delhaye et al. ([11]) focused on the measurement of the surface strains appearing on the fingertip skin under passive shearing. This latter leads to the occurring of strains at the periphery of the contact area, which in turn results in different levels of compression as well as stretch and shear on the contact area. These were dependent on the normal force as well as the direction of the stimulation.

Finally, in 2018, Barrea et al. ([12]) investigated the ability to detect partial slip prior to a full slip under passive movements.

1.5 Aims of the project

The main goal of this master thesis is to compare the force adaptation occuring when manipulating 2 objects with different frictions, on the basis of forces and fingerprints images analyses. To be more precise, as explained in more details in the next sections, an oscillation manipulation was performed with 2 objects exhibiting different frictional conditions, during which forces and fingerprints images at the contact between the index and the object were recorded. Force modulation and adaptation to these two different objects were then analysed, firstly by looking at the data contained in the force signals, before correlating them to possible mechanical clues present on the recorded images.

Another issue to this main objective was also addressed: the influence of the intrinsic fingertip skin moisture level of the subjects on the applied grip force.

2 Material and methods

2.1 Data collection

2.1.1 Participants

Twelve healthy right-handed subjects (9 women and 3 men) aged between 20 and 25 participated in the study.

Two selection criteria were used to accept a subject into the study: having no known motor nor neurological disorder influencing the handling of objects and having the skin of the right thumb and index undamaged (no large scars or cracks).

Before starting the experiment, the written consent of each participant was obtained, after receiving information about the purpose of the research and the details of the manipulations.

2.1.2 Apparatus and setup

During the experiment, the *ActiveTouch* manipulandum has been used. This device, whose mass is 440g and dimensions are 180 x 50 x 52mm, is depicted on Figure 3. It is made up of several components and has to be manipulated by the subjects in precision grip, i.e. held between the thumb and the index. These fingers have to be positioned on small removable glass plates on each side of the manipulandum (see Figure 4). [3]

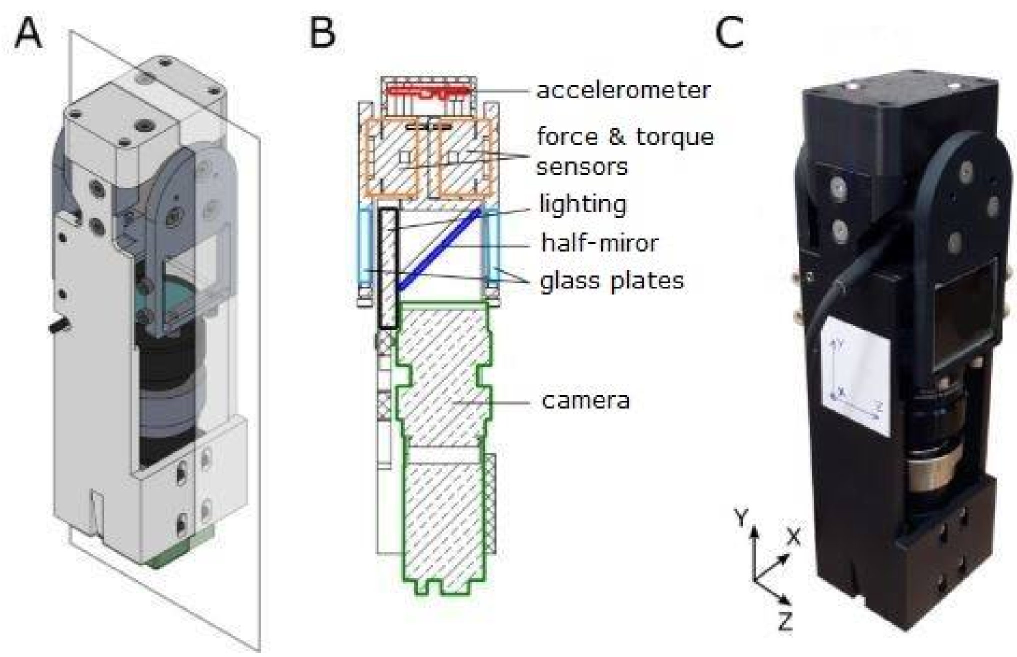

Figure 3: *ActiveTouch* manipulandum. **A**: General description; **B**: Manipulandum section to visualise its main components; **C**: Photography of the manipulandum, with the representation of the reference frame used during data recording. Modified from [3]

Figure 4: The *ActiveTouch* manipulandum held in precision grip. [3]

As shown on Figure 3B, several sensors are embedded in the manipulandum and allow to measure and record data. To be more precise, acceleration of the manipulandum as well as forces and torques applied by each of the two subjects' fingers were recorded throughout the experiment along each of the 3 axes of the reference frame, which is displayed on Figure 3C. The coordinates of the centers of pressure (COP) along the x- and y-axes of both fingers were also recorded. These COP's correspond to the points on the sensors where the resultant forces of the fingers are applied. The acquisition frequency of these signals was 200Hz. [3]

Moreover, an optical system also constitutes the manipulandum. It allows to record images of the fingerprint of one of the two fingers. In this study, the index has been chosen to be the finger whose fingerprint was imaged.
As it can be seen on Figure 5, the functioning of this optical system requires only a half-mirror, an integrated light and a camera: thanks to the half-mirror, on the one hand, the light coming from the lighting system can pass in a straight line to illuminate the fingerprint in contact with the manipulandum, and on the other hand, this image can be deflected so that it is in line with the camera axis and can therefore be correctly recorded.
On the obtained images, the fingerprint appears darker due to diffraction: if the skin is in contact with the plate of the manipulandum, it diffracts the light which is not reflected back to the camera. On the right side of the images is a reference pattern used to compute the relative displacement between the plate on which is positioned the finger and the camera.
The acquisition speed of these images was of 100 frames per second (fps). Their dimensions were 1696 x 1248 pixels (px). This represents an area captured by the camera of 26.5 x 19.5mm (1px $\approx$ 0.016mm). [3]

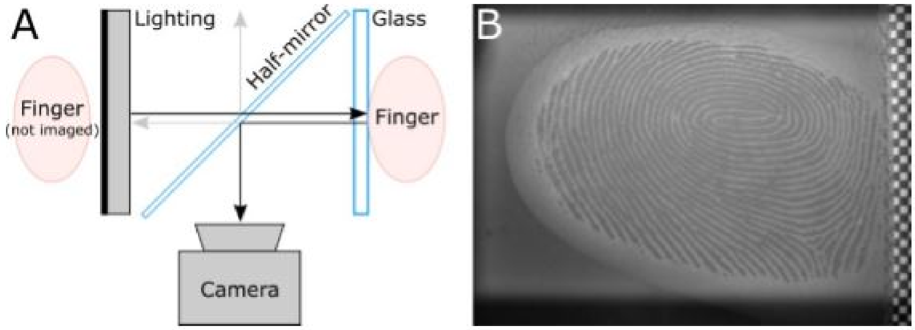

Figure 5: Optical system in the *ActiveTouch* manipulandum. **A**: System operation; **B**: Image captured by the optical system. The fingerprint on it appears darker than the background due to light diffraction. On its right side can be seen the reference pattern. [3]

As aforementioned, the plates on which are positioned the subjects' fingers are removable. It is therefore possible to change them during an experimental session so as to perform manipulations with different friction conditions. The only restriction to this changeability is that the material composing the plates must be transparent to allow the optical system to capture images of the fingerprint. During this study, plates of two different materials were used: glass and nanostructured glass. As its name suggests, the latter is a glass to which a nanoscale surface has been applied. Although the exact manufacturing process of these plates remains confidential, it is known that different methods can be used to make appear the nanostructure on the surface of the glass, including a chemical vapour etching process. [13]

By controlling parameters during the manufacturing process, it is possible to obtain nanostructured glass with more or less nanoscale projection tips (called particles) on its surface. As illustrated on Figure 6, if the number of particles is not too low but not too high, the contact area between the finger and the glass decreases. In this condition, the nanostructured glass is more slippery than normal glass, and this is the reason why it was used in this study. The nanometer size structure is visually imperceptible, it modifies the feel without changing the appearance of the glass, and therefore without subjects noticing it. That represents an advantage. [13]

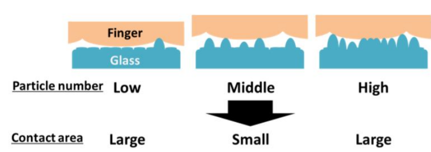

Figure 6: Comparison of the contact area between finger and nanostructured glass with more or less particles at its surface. [13]

For this study, a system of ropes and pulleys was used to totally counterbalance the manipulandum with a counterweight whose mass was 440g. The resulting weight of the system was therefore null, but its inertia was the one of an object twice as heavy, i.e. an object with a mass of 880g. This configuration was set up to perform vertical movements with the manipulandum. [3]

In addition to the manipulandum and the counterweight, the setup also consisted of a moisture sensor (Corneometer CM 825, Courage + Khazaka electronic GmbH) to determine the moisture of the subjects' index. These measurements were performed in the stratum corneum, which is the uppermost layer of the skin. They depend on the dielectric constant measured by the application of an electric field in the stratum corneum when the sensor is brought into contact with the skin. These measurements are arbitrary between 20 and 120, corresponding respectively to a dry or wet skin. [14]

The last components of the setup were an external motion capture system to measure the vertical position of the manipulandum with an acquisition frequency of 200Hz, as well as a metronome and a marking system allowing the subjects to perform their movements at imposed rhythm and amplitude.

2.1.3 Experimental procedure

Ten minutes before starting the manipulations, subjects were asked to wash their hands carefully with soap and water to ensure that no unwanted substances interfered with the results of the experiment. Then, a 10-minute waiting was necessary to allow the natural moisture level of the subjects' skin to recover.
Afterwards, after receiving manipulations instructions and attending a demonstration by the experimenter, each subject had the opportunity to manipulate the manipulandum before starting to record the results, in order to familiarise themselves with the position their fingers had to take on the glass plates as well as to the rhythm of the metronome.

The manipulations consisted of performing vertical oscillations with the manipulandum held in precision grip, with imposed amplitude and frequency. All the subjects being right-handed, they held the manipulandum with their right hand, standing in front of the manipulandum-counterweight setup.

Two blocks of 15 trials were performed by each subject, each trials block corresponding to the use of different glass plates to test different friction conditions: half of the subjects started the experimental session using normal glass, and the other half using nanostructured glass. Both glass plates for both fingers were always of the same type at the same time. The 15 trials of the same block were carried out consecutively. The glass plates were therefore only changed once during the experimental session. The subjects witnessed the change but they were not given any information about the difference between them. They were also unable to see any physical difference between them.

Each trial consisted in the realisation of oscillations of 20cm of peak-to-peak amplitude, following a metronome beeping at 90 beats per minute (bpm) during 30 seconds. At each beat, the manipulandum had to be at one extreme of the oscillation. The metronome therefore beeped 2 times per oscillation cycle. Approximately 20 oscillations were performed per trial.

In total, each subject performed about 600 oscillations (20 oscillations x 15 trials x 2 blocks), including 300 with each type of glass. A total of approximately 7200 oscillations (600 oscillations x 12 subjects) were therefore performed for the purpose of the study.

Before and after each trial, the subjects were asked to measure the moisture level of their index with a sensor, since the moisture content of the skin varies quite rapidly during handling. Moreover, between each trial, the glass plates were cleaned to guarantee the same conditions of friction with the same glass plates throughout the experiment as well as to record images of good quality.

At the end of each trials block, the subjects had to perform a special manipulation to enable the computation of their coefficients of friction. This was also realised with the manipulandum held in precision grip, but this time it remained static (the subjects immobilised it with their left hand). For each type of glass plates, the subjects had to carry out 3 trials of 30 seconds during which vertical back-and-forth movements at the surface of the plates were done, as shown, with respect to time, on Figure 7. During each of the 3 trials, subjects were asked to apply different normal forces to the surfaces: a weak force between 0.5-1N and 3N, a medium force between 3N and 5N, and a large force between 5N and 8-9N. They could see the force they were applying to the manipulandum on a screen in front of them. During these particular trials, only data signals were recorded, without any images. [15]

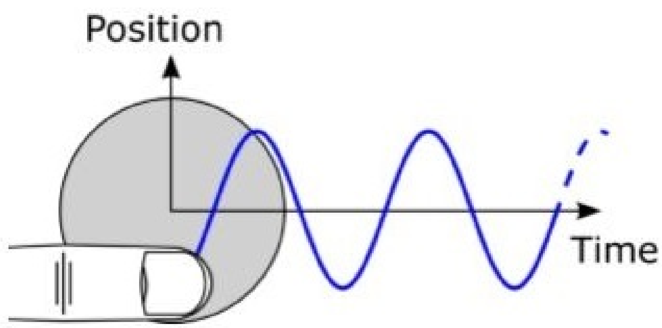

Figure 7: Method to estimate the static coefficient of friction in precision grip: trajectory of the thumb and index on the sensor of the manipulandum during the back-and-forth movements. [15]

2.2 Data analysis

Data signals (force, position, acceleration and COP signals), moisture measurements and images were processed using Matlab. Many functions that were previously developed to process data collected during manipulation with the *ActiveTouch* manipulandum were used in this study. These are available in the *LibactiveTouch*, *Imagetools* and *Matlabutils* toolboxes.

2.2.1 Data signals

As already explained, when manipulating objects, the force acting on the contact surface between the fingertip and the object can be divided into 2 components: the grip force and the load force. In the recorded signals, this decomposition was automatically decomposed into these 2 components, as depicted on Figure 8. [3]

- The grip force (GF) was computed as the average of the normal forces applied by both fingers on the manipulandum.

$$GF = \frac{GF_{thumb} + GF_{index}}{2}$$

- The load force (LF) was obtained by computing the resultant force of the ones tangentially applied by both fingers on the manipulandum. Its horizontal (LFh) and vertical (LFv) components are its decomposition along the x- and y-axes and correspond to the sum of the horizontal or vertical tangential forces exerced by both fingers on sensors.

$$LFh = LFh_{thumb} + LFh_{index}$$

$$LFv = LFv_{thumb} + LFv_{index}$$

$$LF = \sqrt{LFh^2 + LFv^2}.$$

  As aforementioned, the load force normally results from the gravitational and inertial forces of the object ($LF = mg + ma$). In the present case, the weight of the object being fully compensated, the load force depends only on the acceleration of the object, considering its double mass (sum of the masses of the object and the counterweight).

Figure 8: Decomposition of the force applied by the fingers on the manipulandum into grip force (GF) and load force (LF). [3]

Before the analysis, all signals recorded during the experiment were filtered with a 4^{th} order low-pass filter. The forces, accelerations and positions were filtered with a filtering frequency of 40Hz, while the filtering frequency for the center of pressure signals was of 10Hz. This step is indeed essential so as to suppress parasitic noise present in the data.

Based on the signal of the vertical manipulandum velocity, which was obtained by deriving its vertical position signal with a sample frequency of 200Hz, the segmentation of all the data into oscillations was performed. To be more precise, positive peaks in the vertical velocity signal were detected and defined as the beginning of the oscillations. From a vertical position point of view, these peaks correspond to the middles of the trajectory between the minima and the maxima of the movements. This particular point is therefore considered to be the origin of the reference frame used for the analysis, with the position being positive when the manipulandum was moving towards its highest position. As a result, as shown on Figure 9, an oscillation starts at the middle between the minimum and the maximum of the movement amplitude and ends once a full cycle of the oscillation has been completed (initial position - maximum - minimum - back to initial position). After this segmentation, a total of 7034 oscillations was counted.

So as to ensure a comparable and reliable sample of oscillations across all subjects, selection criteria had to be applied.

- The duration of each oscillation had to be neither too short nor too long. This criterion verified that the subjects respected the rhythm of the oscillations imposed by the metronome.
- The kinematics of the movements was also investigated, to ensure that it was fairly constant across all trials and all subjects. This criterion verified that the subjects respected the imposed amplitude of the oscillations.
- The vertical load force at the starting point of the oscillations had to be close to 0N (between -0.8 and 0.8N), since the mass of the manipulandum was totally counterbalanced.

After validation of the oscillations based on these selection criteria, 6739 valid oscillations were kept for signal-based analysis, including 3370 performed with the normal glass and 3369 with the nanostructured glass.
On Figure 9, an example of the segmentation of some signals into oscillations is shown. As the rhythm of these oscillations seams regular as well as their kinematics, and since their initial vertical load force is close to 0N, all the presented oscillations meet the selection criteria and were all kept for further analysis.

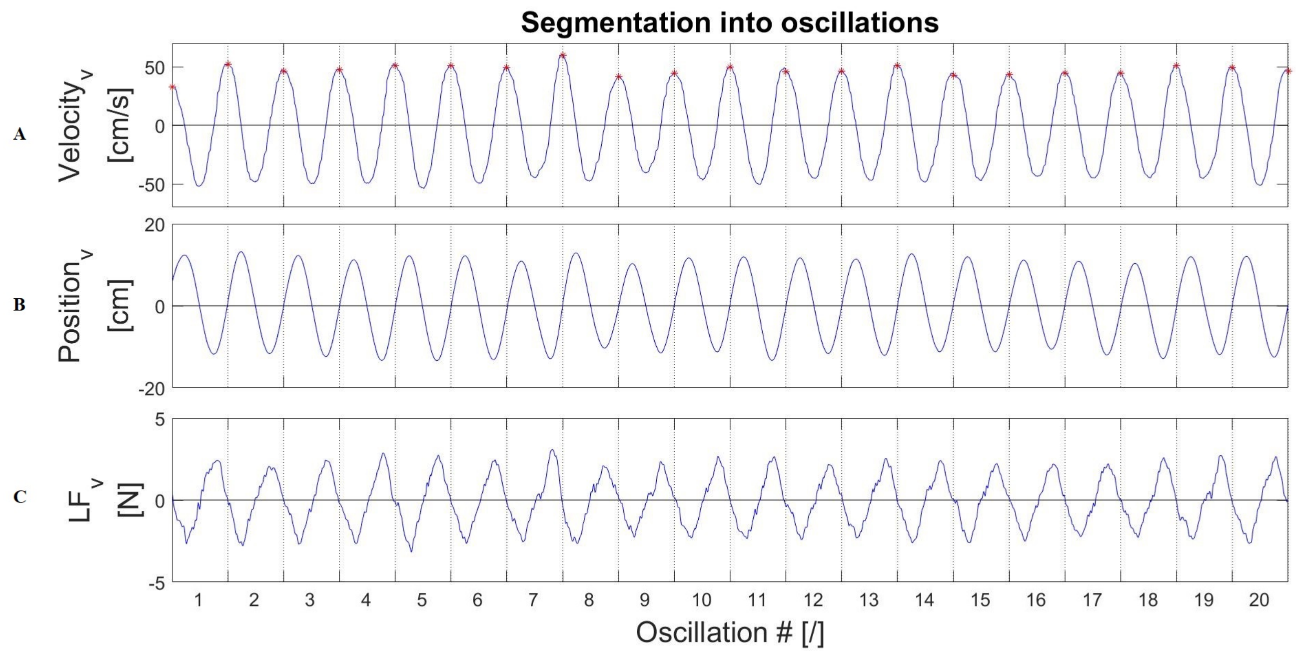

Figure 9: Signals segmentation into oscillations. The x-axis represents number of oscillations segmented into a trial. Each vertical doted line defines an oscillation. The data represented on this figure is the data recorded during the second trial of the first subject. **A**: Vertical velocity of the manipulandum in cm/s. Red asterisks represent the detected peaks marking the beginning of each oscillation. **B**: Vertical position of the manipulandum in cm. Each oscillation begins in the middle position before reaching the maximum of its trajectory, then its minimum and returning to the initial position. **C**: Vertical load force applied by the subject on the manipulandum in N. Initial value of each oscillation is close to 0N.

Finally, the load and grip forces recorded during the particular manipulations at the end of each trials block were used to compute the coefficients of friction for both glasses and both fingers.

The coefficient of friction is of particular interest since, with the load force, it determines the grip force slip, i.e. the minimal grip force to apply to avoid slipping of the held object (SlipF = $\sqrt[n]{\frac{LF}{2k}}$, defined for both sensors, with n and k defined by the coefficient of friction). Although it has been often considered as constant, it non-linearly varies with low values of grip force (below 5N). By asking to the subjects to perform 3 times the same manipulations for grip forces between 0.5N and 8-9N, it was therefore possible to ensure that all possible variations in this coefficient were handled. It has to be noted that the glass is a particular material for which the static and dynamic coefficients of friction are equal. This is why, only mentions of "coefficient of friction", which is also depicted as μ, is used in this report.

The coefficient of friction is defined as the ratio between the friction and grip forces, i.e. the ratio between the tangential force to the surface which is needed to break the bonds between the fingertip and the surface and which therefore leads to the slipping of the object and the grip force. It therefore corresponds to the ratio between load and grip forces when the held object starts slipping.

To compute it, it is therefore required to detect the slip onsets. These can be found by looking at the maximum values of the ratio between the load and grip forces just after that the vertical position of the center of pressure reached an extreme value (minimum or maximum). Indeed, when the center of pressure reached an extreme value, the finger was switching from a back to a forth movement (or vice versa), which means that a slip had to occur. At each slip onset, a discrete value of the coefficient of friction was found and then, a negative power law ($\mu = k\ (GF)^{\ n-1}$) was applied on these discrete values, allowing the coefficient to be expressed as a continuous function of the applied grip force varying between ~0.5 to ~9N.

The obtained results for the 4 coefficients of friction for each subject (for both fingers and glasses) are depicted and further analysed in Section 3.

The signal analysis carried out in this study mainly focuses on the evolution of the grip force, its modulation as well as the safety margin.

2.2.2 Fingerprint images

So as to exploit the data contained in the images of the fingerprints, they first had to be processed. As the signals, images were segmented into oscillations on the basis of the peaks found in the vertical velocity signal of the manipulandum. Since the recording speed of the images was of 100 fps and that the metronome beeped at 90 bpm (with 2 beeps per oscillation cycle), oscillations were composed of 149 images in average.

The first step in the analysis of the images was to detect the contact area (CA) between the finger and the glass plate. This contact area is defined as all the points of the fingertip skin which are in contact with the plate as well as the ones situated in the valleys between the ridges in contact with the plate. The contact area is not constant along an oscillation cycle: at the beginning of the latter, it is usually ellipse-shaped, but it tends to deform and reduce when tangential forces appear.
The contact areas throughout the oscillation cycle were obtained thanks to an algorithm previously developed using machine learning. It was therefore necessary to manually detect them on a small sample of images from all subjects. The algorithm then learned and trained a model on

the basis of this small sample before determining the contact areas on the entire set of images. The operating principle of this algorithm is to apply mathematical morphological operations (closing and opening) based on the grey value of the image pixels in order to make the ridges and valleys of the fingerprint a single area. The obtained fingerpad zone was then separated from the background and an ellipse was fitted to a sample of points distributed between the two identified regions to obtain the contact area. [3] [10]
An example of a detected contact area on an image is shown on Figure 10A-B.

At this point of the image analysis, all the oscillations meeting the signal-based selection criteria were considered, i.e. 6739 oscillations out of the 7034 initially detected. In order to ensure the quality of the contact area obtained using the algorithm, a visual check of them was performed. As a result, some oscillations were discarded. As shown on Figure 10C and Figure 10D, some oscillations were suppressed from the samples due to poor contact area detection. This can be due to a lack of contrast between the grey values of the pixels in contact or not with the glass plate, or due to the fact that the fingerprints were situated in an extreme part of the glass plate. After the visual check of the contact area, the total count of oscillations available for the images analysis was 6115. The visual check enabled to confirm that oscillations considered valid on the basis of the signals selection criteria were oscillations during which index was correctly placed on the glass plate. The friction conditions during these manipulations were therefore those reflected by the computed friction coefficients.

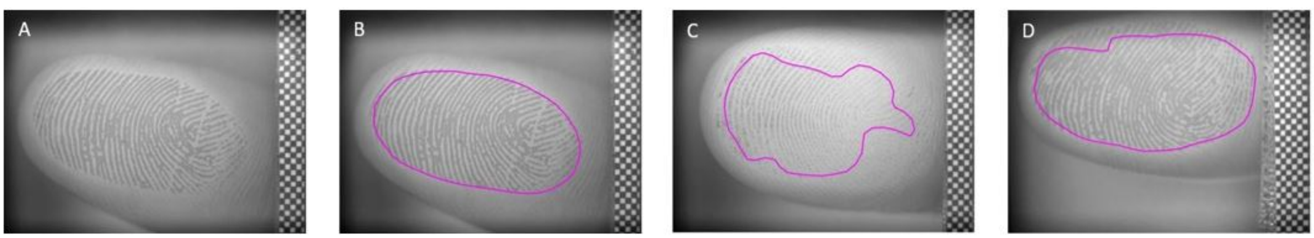

Figure 10: Contact area detection on fingerprints images. **A**: Image of the index of one subject captured during manipulation. **B**: Image A on which the contour of the detected contact area is depicted in pink. **C - D**: Rejected images for image analysis because of poor detection of the CA contour.

Images were then analysed to compute the displacement field inside the contact area along all the oscillation cycle. The interest of this computed variable is to detect sliding of the fingertip on the glass plate.
The displacement field was obtained by using the optical flow method. Optimal feature points were first detected in the contact areas on 3 distinct frames for each oscillation: the first frame, the last frame and the frame in the middle of the oscillation. Their position were then tracked from frame to frame, from the first to the last frame, from the last to the first frame and from the frame in the middle of the oscillation to the first and to the last frames of the oscillation. These different trackings of feature points enabled to take into account feature points that appear or disappear in the contact areas due to the deformation of the skin and the gain or loss of contact between the fingertip and the plate. Looking at the displacement of these feature points from frame to frame enables to obtain the displacement field. [11]
An example of feature points used to compute the displacement field is shown on Figure 11.

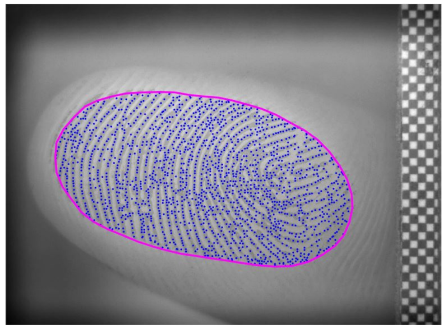

Figure 11: Computation of the displacement field in the CA between the index and the glass plate on the images. The image is the same as the one on which the contact air detection has been shown previously. The pink line is the contact area border and the blue points are the feature points which are tracked from frame to frame to compute the displacement field.

As aforementioned, the interest of the computation of this variable is to detect if some sliding of the fingertip on the glass occurs during the oscillation manipulation.
In the present study, it enabled to detect the minimal vertical displacement of the feature point that moved the least vertically between the first and the last frames of each oscillation cycle. If the minimal vertical detected displacement is null, this means that at least one point of the contact area did not slide on the plate during the oscillation cycle. In other words, this means that there was no full slip of the fingertip on the plate during the oscillation movement. It has to be mentioned that a minimal displacement of 1 px (or 0.016 mm) is often required to consider it as a non-stuck point. [3]

The last point of the images analysis was the computation of the fingerpad surface strains. So as to obtain them, strain rates were first obtained by deriving them from the displacement field from frame to frame obtained at the previous step, using the Green-Lagrange equations. To be more precise, after triangulating the contact area on the first frame of the oscillation with triangles having the feature points as center, a displacement field gradient was estimated for each triangle on the basis of the shift of each of their vertices. Strains rates, which are composed of 3 components, i.e. the axial strain rate component along the x-axis ε_{xx}, the axial strain rate component along the y-axis ε_{yy} and the shear strain rate component ε_{xy}, were then derived according to the following equations in which the u and v are the displacements respectively along the x- and y-axes, and attributed to the centers of each triangles.

$$\varepsilon_{xx} = \frac{\partial u}{\partial x} + 0.5\left[\left(\frac{\partial u}{\partial x}\right)^2 + \left(\frac{\partial v}{\partial x}\right)^2\right]$$

$$\varepsilon_{yy} = \frac{\partial v}{\partial y} + 0.5\left[\left(\frac{\partial u}{\partial y}\right)^2 + \left(\frac{\partial v}{\partial y}\right)^2\right]$$

$$\varepsilon_{xy} = 0.5\left(\frac{\partial u}{\partial y} + \frac{\partial v}{\partial x}\right) + 0.5\left(\frac{\partial u}{\partial x}\frac{\partial u}{\partial y} + \frac{\partial v}{\partial x}\frac{\partial v}{\partial y}\right)$$

Compression of the fingertip corresponds to negative axial strains whereas positive axial strains correspond to dilation of the fingertip. With respect to shearing strain, it is defined as positive if the angle between the positive x and y-axes decreases, and as negative otherwise.
In this study, the evolution of strain rates along the oscillation cycle were analysed. To obtain

the total strains, i.e. the deformation of the fingerpad relative to it on the first frame of the oscillation, it would have been necessary to sum the strain rates cumulatively along all frames of the oscillation cycle. [11]

A representation of strain rates computed on 1 image is represented on Figure 12. A more detailed analysis of the strain rates evolution along an oscillation cycle is made in Section 3.

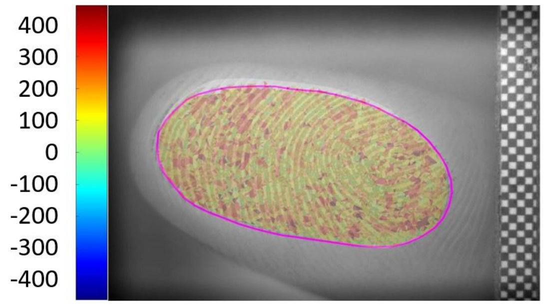

Figure 12: Computation of the strain rates in the CA between the index and the glass plate on the images. The image is the same as previously shown. The pink line is the contact area. Dilation is represented by positive values, whereas negative values represent compression.

A decomposition of the strain matrix ε into principal strains was finally carried out. This transformation corresponds to applying a rotation on the reference frame so as to cancel the shear strain component. By doing this, the maximum values of tensile and compressive strains, corresponding respectively to the principal strains e_1 and e_2, were obtained. From a mathematical point of view, the decomposition of the strain matrix ε is the following, with $\mathbf{v_1} = (v_{x1}, v_{y1})$ and $\mathbf{v_2} = (v_{x2}, v_{y2})$ being the orthogonal eigenvectors ($\mathbf{v_1}.\mathbf{v_2} = 0$) and e_1 and e_2 being the eigenvalues [11]:

$$\underline{\underline{\varepsilon}} = \begin{bmatrix} \varepsilon_{xx} & \varepsilon_{xy} \\ \varepsilon_{xy} & \varepsilon_{yy} \end{bmatrix} = \begin{bmatrix} v_{x1} & v_{x2} \\ v_{y1} & v_{y2} \end{bmatrix} . \begin{bmatrix} e_1 & 0 \\ 0 & e_2 \end{bmatrix} . \begin{bmatrix} v_{x1} & v_{x2} \\ v_{y1} & v_{y2} \end{bmatrix}^{-1} .$$

The strains analysis performed in this study focused mainly on the evolution of the main components during the experimental session.

2.3 Statistical analysis

So as to quantify the observations made on the results, statistical tests were carried out, also using Matlab. These consisted in paired t-tests as well as t-tests, with the use of the traditional 5%-value to determine their statistical significance. The use of one of the other type of t-tests was dependent on the evaluated situation. These tests are usually used to compare averages of respectively paired, or not, samples differing by some conditions.
In this study, the different compared conditions were the different types of glass. Statistical tests were also performed within each trials block and within trials to assess the force adaptation with practice.

3 Results

This section is divided into several parts corresponding to the various data that have been analysed. First of all, the coefficients of friction and moisture evolution data are presented. Kinematics and dynamics of the oscillation movements are then introduced before reviewing results obtained on the basis of the acquired images.

Most of the aforementioned parts are often divided into several points. After displaying the general figure of the analysed variable throughout the entire experimental session and making some general comments about it, a first quantitative approach of the parameter is given by computing its averaged values on each trials blocks for each subject. Then, as some adaptation in the behaviour of the subjects can occur, an analysis of the parameter evolution within each trials block is performed, by comparing the values of the parameter on the 3 first and last trials of each trials block. On the same principle, the parameter evolution within trials was also investigated, but this time by comparing the 3 first and last oscillations of the trials. This was thus done for each type of glass and then, a comparison between the 2 glasses was made, by using paired t-tests. The averaged value of the parameter in both trials blocks, as well as its evolution within the trials block and its evolution within trials were compared in the 2 glasses conditions. The comparison of the evolution within the trials block and within trials were performed by comparing differences. The latter were either the difference of the parameter value between the 3 last and first trials of the same trials block, or the difference of the parameter value between the 3 last and first oscillations of all trials in the same trials block.

As the fingertip skin moisture is known to have an impact on the coefficient of friction, and therefore on the grip force, its influence on the latter was investigated. So as to do it, different correlations between moisture measurements and other parameters were performed. The results are presented in each subsections of the concerned parameters.

In most cases, the data for all the subjects are represented separately in order to detect possible different behaviours between them but if a generalisation can be made, this is reported.

Finally, it is useful to take note of these few remarks concerning the presentation of its rather complex data, in order to make it easier to read.

- When a figure contains 12 subfigures representing data for all the subjects, the 6 first subfigures of the 2 first columns are always the data concerning the subjects that began the experimental session by performing oscillations using the normal glass plates. As a result, the 6 last subfigures correspond to the subjects which began manipulations with the nanostructured glass plates. On the figures, the data relating to manipulations with the normal glass are always depicted in red, and those relating to oscillations performed with the nanostructured glass are drawn in blue.
- In the tables and when giving the p-values, the normal glass is depicted by the "N.G." abbreviation, whereas "NS.G." stands for the nanostructured glass.

3.1 Coefficients of friction

As explained in details in Section 2, the coefficients of friction (μ) for both the thumb and the index, and each type of glass for each subject were computed. The obtained results are depicted on Figure 13 for the thumb coefficients, and on Figure 14 for the index coefficients. The values obtained for the k and n fit parameters are available in Table 1 and in Table 2. As a remainder, μ can be expressed as a function of the grip force following a negative power law: $\mu = k\ (GF)^{\ n-1}$.

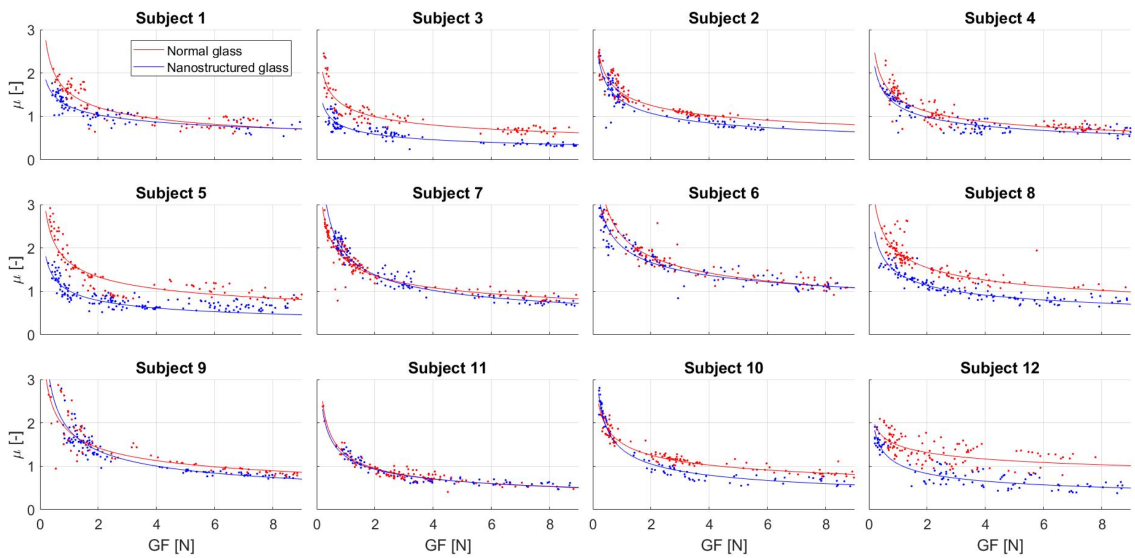

Figure 13: Computed coefficients of friction for each subject and both types of glass, on the basis of the force recorded at the thumb sensor. Red lines and dots refer to the normal glass, blue lines and dots refer to the nanostructured glass.

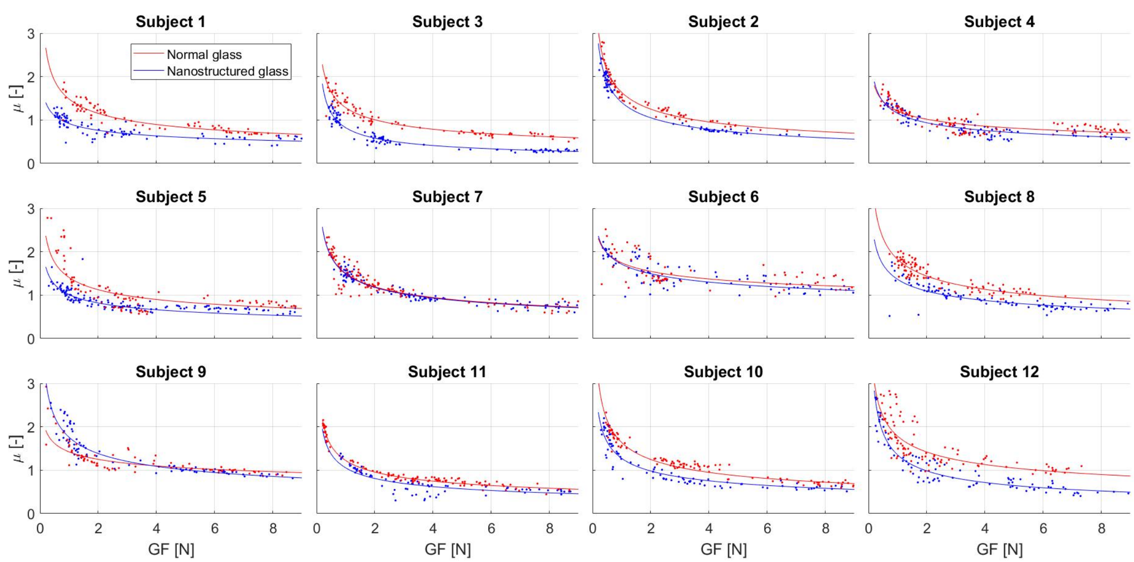

Figure 14: Computed coefficients of friction for each subject and both types of glass, on the basis of the force recorded at the index sensor. Red lines and dots refer to the normal glass, blue lines and dots refer to the nanostructured glass.

Subject #	1	2	3	4	5	6	7	8	9	10	11	12
N.G. - k	1.55	1.54	1.23	1.42	1.67	2.28	1.72	1.90	1.80	1.53	1.27	1.49
N.G. - n	0.64	0.71	0.69	0.65	0.67	0.66	0.67	0.70	0.67	0.71	0.58	0.83
NS.G. - k	1.23	1.35	0.75	1.24	1.01	2.03	1.86	1.42	1.84	1.39	1.22	1.05
NS.G. - n	0.75	0.66	0.65	0.66	0.64	0.71	0.57	0.68	0.56	0.59	0.60	0.66

Table 1: Fit parameters computed to express the coefficients of friction in terms of the grip force. Parameters for the thumb coefficients of friction and for both types of glass.

Subject #	1	2	3	4	5	6	7	8	9	10	11	12
N.G. - k	1.48	1.64	1.29	1.21	1.41	1.74	1.50	1.82	1.42	1.64	1.22	1.78
N.G. - n	0.64	0.61	0.65	0.75	0.68	0.83	0.67	0.66	0.81	0.61	0.64	0.67
NS.G. - k	0.92	1.41	0.82	1.16	1.01	1.71	1.49	1.36	1.76	1.27	1.05	1.35
NS.G. - n	0.73	0.58	0.50	0.70	0.70	0.80	0.66	0.68	0.65	0.62	0.62	0.54

Table 2: Fit parameters computed to express the coefficients of friction in terms of the grip force. Parameters for the index coefficients of friction and for both types of glass.

The first observation that can be made is that, overall, the coefficients of friction for the normal glass are higher than those of the nanostructured glass at the same values of normal force for all the subjects. This is consistent with the fact that nanostructured glass is more slippery than normal one.

The only subject for whom this affirmation is not true is the subject 9 for the index. This can be explained by the fact that only very few discrete low-GF points were detected for the calculation. This therefore made it difficult for the program to obtain consistent coefficient values in this very low GF area when applying the negative power law, at least as far as normal glass was concerned. For this reason, and also because as shown in Table 1 and Table 2 the values of the fit parameters obtained for the two coefficients of the two fingers were very close, the decision was made to use only the friction coefficients calculated for the thumb of the subjects for further analyses. As mentioned in [15], the coefficients of friction obtained for both fingers are often very close, resulting in the fact that the dependence of μ on the grip force can be captured by the computation of only the coefficient of friction of one of the two fingers.

The second interesting observation is that, as expected, all their values seem to stabilise at higher grip force values (from 5-6 N). This corresponds to the literature on the subject. [15]

3.2 Moisture evolution

As a reminder, moisture measurements were performed before and after each trial of oscillations. They can range between 20 and 120 in arbitrary units. Figure 15 depicts these measurements for all the subjects across the 30 trials they performed.

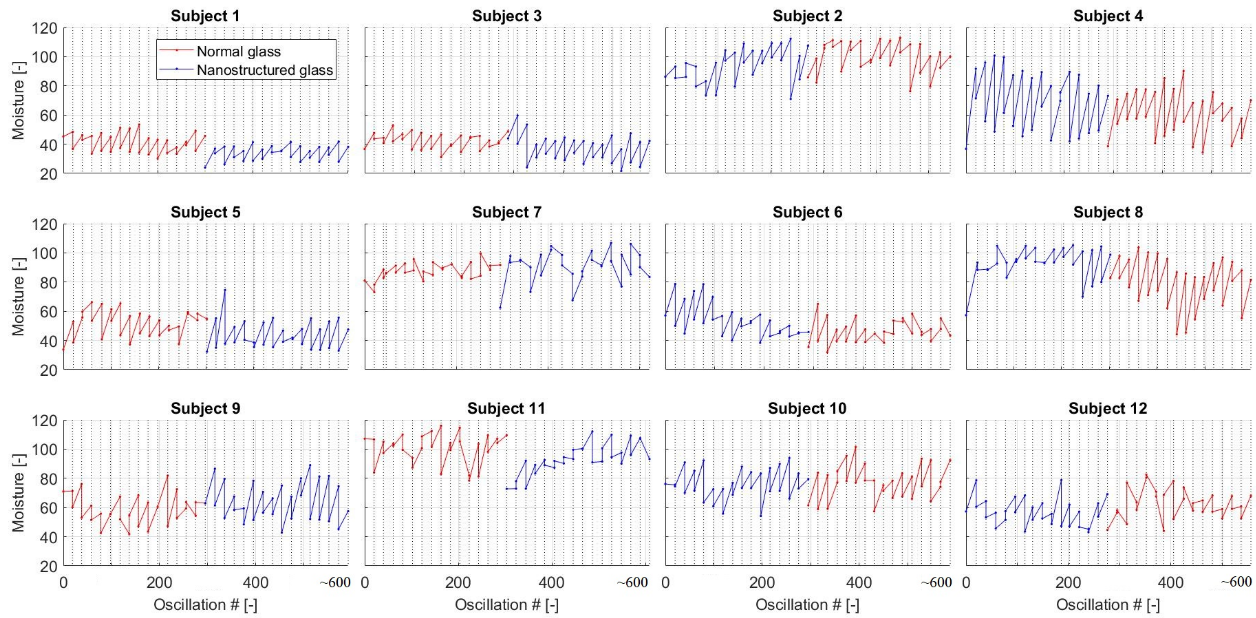

Figure 15: Moisture measurements for all the subjects across all trials. Red lines refer to the normal glass, blue lines refer to the nanostructured glass. Vertical black doted lines delimit the trials.

It can be seen on Figure 15 that subjects have a mean moisture level which is specific and can be rather low, medium or high, corresponding respectively to a dry, moist or wet skin. To quantify their respective moisture level, the average of their measurements for both types of glass separately and then combined were computed and are available in Table 3. Based on these values, a categorisation of the subjects into 4 groups can be made based on the categorisation made in [16]. As the mean moisture of the subjects 1 and 3 was below 45, they have a dry skin. Subjects 4, 5, 6, 9 and 12 have a normal skin (mean moisture level between 45 and 70). The skin of the subjects 7, 8 and 10 is moist since their moisture measurements are between 70 and 95 and finally 2 subjects have a wet skin, i.e. a mean moisture level higher than 95.

Subject #	1	2	3	4	5	6	7	8	9	10	11	12
N.G.	41.10	100.02	42.32	61.10	51.78	46.46	87.48	79.61	59.03	77.42	100.56	62.61
NS.G.	34.09	93.88	37.25	69.45	43.98	53.45	91.03	93.02	64.15	75.94	93.35	56.85
Both types of G.	37.59	96.95	39.79	65.28	47.88	49.95	89.26	86.31	61.59	76.68	96.95	59.73

Table 3: Means of the moisture measurements for both types of glass and all the subjects. The units of moisture measurements are arbitrary units.

Regarding the evolution of skin moisture within each trials block, it seems rather stable. The only subjects for whom a statistical difference is observed are the 6 and the 11, considering only the measurements using the nanostructured glass. But for both subjects, the trend is not the same: the moisture tends to decrease across trials with nanostructured glass for subject 6 whereas an it tends to increase for the subject 11. These intra-block variations are not confirmed for the population in both normal and nanostructured glass blocks (p-value$_{N.G.} = 0.52$ and p-value$_{NS.G.} = 0.50$).

The moisture evolution within trials is also of interest: an increase in the moisture measurements takes place between almost all beginnings and ends of each trial for all the subjects and both types of glass. This reflects the occlusion phenomenon, due to the accumulation of the moisture secreted by sweat pores at the interface between the fingertip and the held object. A quantification of this systematic raise was performed for each subject and each type of glass separately by computing the average percentage of increase between the first and second moisture measurements of each trial. The resulting values are available in Table 4.

Subject #	1	2	3	4	5	6	7	8	9	10	11	12
N.G.	28.06	14.45	18.84	51.13	23.93	11.18	-0.77	38.03	16.32	22.63	9.89	3.31
NS.G.	26.96	16.31	45.41	64.22	42.07	24.63	4.47	13.31	37.55	22.61	5.67	22.97

Table 4: Mean percentages of increase in moisture within trials due to occlusion phenomenon, for both types of glass and all the subjects.

Although this occlusion phenomenon is well marked for some subjects, it appears to be non statistically significant for subjects 6, 7 and 12 using the normal glass and for the subject 7 using the nanostructured glass. The subject 7 seems therefore to have a less pronounced occlusion phenomenon, regardless of the glass condition, which is confirmed by looking at the curves displayed on Figure 15.
Not surprisingly, the effect of this occlusion phenomenon appears to be statistically significant at the population level for both types of glass (p-value$_{NG.} = 5.67\ 10^{-04}$ and p-value$_{NS.G.} = 7.36\ 10^{-05}$).

The accumulation of the moisture at the fingertip-object interface is known to result in the plasticisation of the outer layer of the fingertip skin, leading to making it softer. It therefore modifies the mechanical properties of the fingerpad, and is therefore a key parameter in the analysis of the force adaptation during precision manipulations. [17]

Comparison between both glasses

No significant difference computed on the population was observed between both types of glass, whether between the mean value of moisture per trials block (p-value = 0.89), its evolution within blocks (p-value = 0.79) or within trials (p-value = 0.21). However, at the individual level, 5 subjects (subjects 3, 6, 8, 9 and 12) present a statistical difference in their moisture adaptation within trials between both glasses. (Example given, on Figure 15, subject 8: it can clearly be seen that the occlusion phenomenon is much more pronounced during the second trials block).

3.3 Correlation between moisture and coefficients of friction

On the basis of the presented variables so far, a simple correlation was made based on the data collected from subjects to observe the relation between the moisture and the coefficients of friction. The result is depicted on Figure 16.

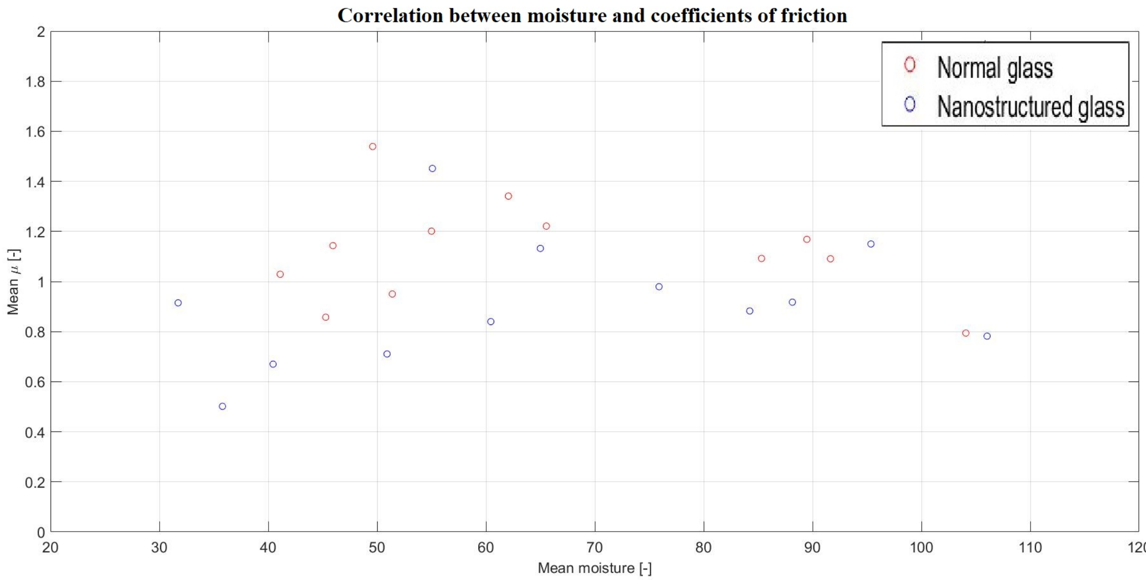

Figure 16: Correlation performed between coefficients of friction and mean moisture measurements for all the subjects. Red points refer to normal glass whereas blue points refer to nanostructured glass.

The trend on Figure 16 is consistent with what is presented in the literature: there is an intermediate moisture level at which the coefficient of friction is maximum. Indeed, it can be observed that at low and high values of moisture, the values of the coefficients of friction decrease. In the reference paper [18], the optimum humidity was around 7 on a scale of 4 to 10, which would roughly correspond to an index of 70 on the used moisture scale in this study. In the present case, the optimum coefficients of friction are situated to slightly lower moisture values.

3.4 Kinematics and dynamics

3.4.1 Standard trial

Before focusing on the evolution of particular variables (i.e. grip force, grip force modulation and safety margin), it is interesting to look at what the force signals look like in a standard trial.

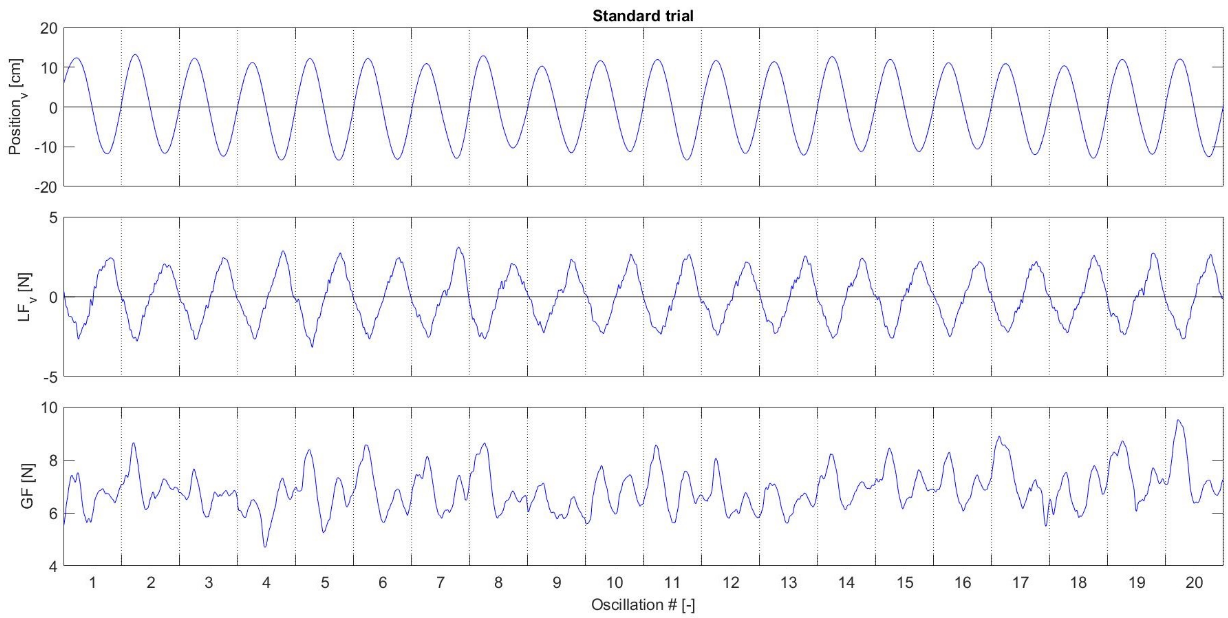

Figure 17: Vertical position [cm], vertical load force [N], and grip force [N] during a standard trial. Vertical black doted lines delimit the oscillations.

As described in Section 2, the segmentation of the oscillations was performed so that the first movement of the oscillations cycle was upwards. As expected, the vertical load force reached therefore first its minimal value over the cycle. Moreover, the vertical load force is oscillating around 0N as the manipulandum was fully counterbalanced. It is therefore only composed of its inertial part, and varies depending on the vertical acceleration of the manipulandum. [19]

With regard to the grip force, it can be seen on Figure 17 that its value is not constant but continuously modulated. So as to prevent the slipping of the object, the grip force has to always be greater than the slip force, which depends on the load force and the coefficient of friction. It is therefore modulated by the change in load force.
A last remark about Figure 17 is that the coupling between grip and load forces seems of good quality. This can be explained by the fact that the movements were totally predictable, without any unexpected perturbation during the manipulations. [20]

3.4.2 Grip force evolution

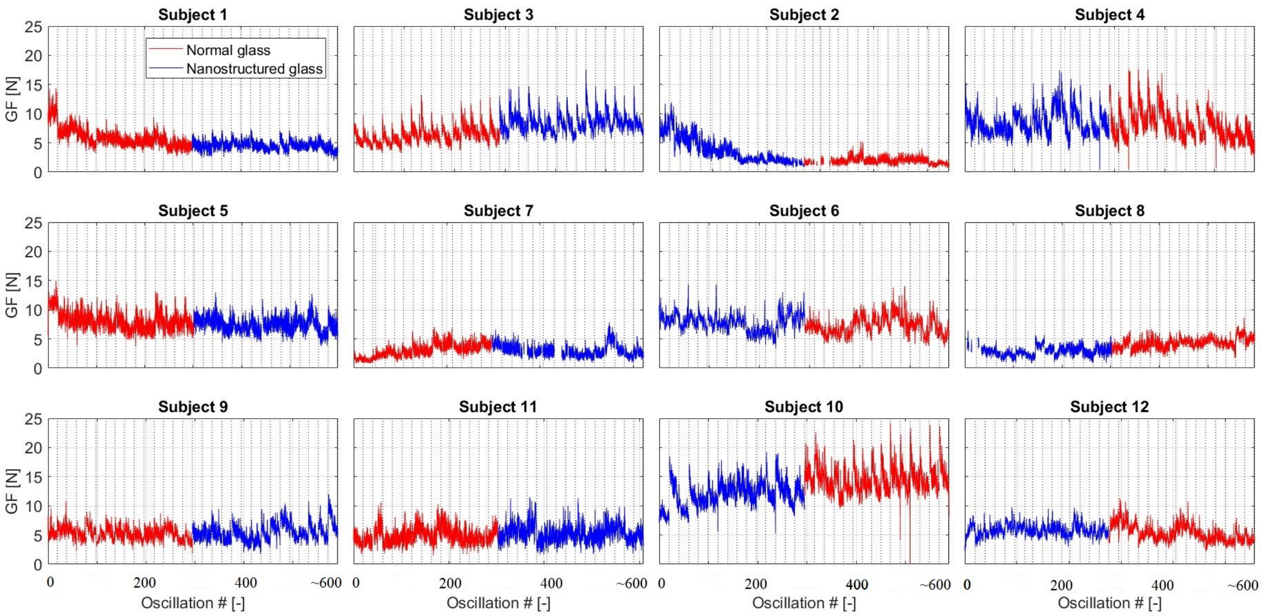

Figure 18: Evolution of the grip force [N] across all the trials of all the subjects. Red lines refer to the normal glass, blue lines refer to the nanostructured glass. Vertical black doted lines delimit the trials.

From a general point of view, it can be seen on Figure 18 that the grip force is a variable that fluctuates a lot amongst all subjects, trials blocks and oscillations. The study of its adaptation over time is therefore crucial.

At first, the data on the mean level of the grip force are available in Table 5.

Subject #	1	2	3	4	5	6	7	8	9	10	11	12
N.G.	5.96	1.94	6.26	7.94	8.08	7.30	2.98	4.34	5.26	14.53	4.97	5.26
NS.G.	4.61	3.72	8.52	8.47	7.45	7.83	3.00	2.96	5.51	11.98	5.29	5.76

Table 5: Means of grip force values [N] for each subject and both types of glass.

For the same carried out manipulation, some subjects deployed a quite low grip force (e.g. subjects 2, 7 and 8) whereas the grip force deployed by some others was quite high (subject 10).

Depending on the subjects, the variation within a trials block can be considerable or not: the grip force of the subjects 1, 3, 7 and 12 varied significantly when using the normal glass, whereas only the subject 2 changes significantly the grip force when using the nanostructured glass. Once again, different trends are seen in the subjects' population. Comparing the subject 1 and 3, it is clear that the first one tends to decrease its grip force when performing oscillations with the normal glass, whereas the trend observed by the subject 3 is an increase. At the population level, no statistical trend was observed, for each type of glass (p-value$_{N.G.} = 0.34$ and p-value$_{NS.G.} = 0.48$).

The greatest variation of grip force across all the experimental sessions seems to occur within trials. Usually, if an adaptation of the grip force is made within trials, the applied grip force at the beginning of a trial tends to be higher than at its end. This adaptation is confirmed for 6 subjects (subjects 1, 3, 4, 5, 9 and 10) for both glasses, as well as for the subjects 2 and 6 for the manipulations realised with respectively the nanostructured and the normal glass. This trend is confirmed by statistics at the population level (p-value$_{N.G.}$ = 0.03 and p-value$_{NS.G.}$ = 0.01). This suggests that even in subjects for whom statistical significance was not confirmed, the same trend can probably be observable in their data.
This change in grip force could be due to rapid adaptation to the performed task due to repetition, as well as moisture changes. This last point is studied at the end of this section about the grip force.

Comparison between both types of glass

At the level of the population, comparing the two types of glass, there was no statistical difference in the average grip force applied in each block, nor within a block, nor within trials.
However, at the individual level some differences were observed. Indeed, a statistical difference in the evolution of the grip force between both types of glass was found for 4 subjects (subjects 2, 7, 8 and 12) within trials blocks, and a more marked trend was observed for the comparison of the adaptation within the trials for 7 subjects (subjects 1, 3, 4, 5, 6, 9 and 10).
It is interesting to note that 6 subjects out of these 7 ones are subjects for which an adaptation within trials for both glasses was observed. This means that they adapted their behaviour for both glasses but not in the same way.

Influence of the moisture level on the grip force

As aforementioned, some correlations between moisture measurements and variables were computed so as to detect a relation between them.

Firstly, a separated correlation for each subject was performed between the mean grip force applied per trial and the 30 means of their moisture measurements. For none of the subjects, this correlation was significant, not leading to a linear relationship between the evolutions of the grip force and of the moisture level within each trials block.
Taking this result into account, as well as the fact that the moisture measurements did not vary significantly within the trials blocks, it can be argued that the adaptation of the grip force within a trials block was probably more related to a habituation caused by the repetition of the task.

However, by placing the same points as previously described but on the same plot for all subjects, an interesting trend can be observed (see Figure 19): the applied mean grip force tends to decrease for higher moisture levels, except for subjects 4 and 10 (depicted by some asterisks on Figure 19). Excepting the data from these two subjects, this trend is consistent with what is found in the literature: there is an optimal moisture level that minimises grip force and maximises the coefficient of friction. [18]

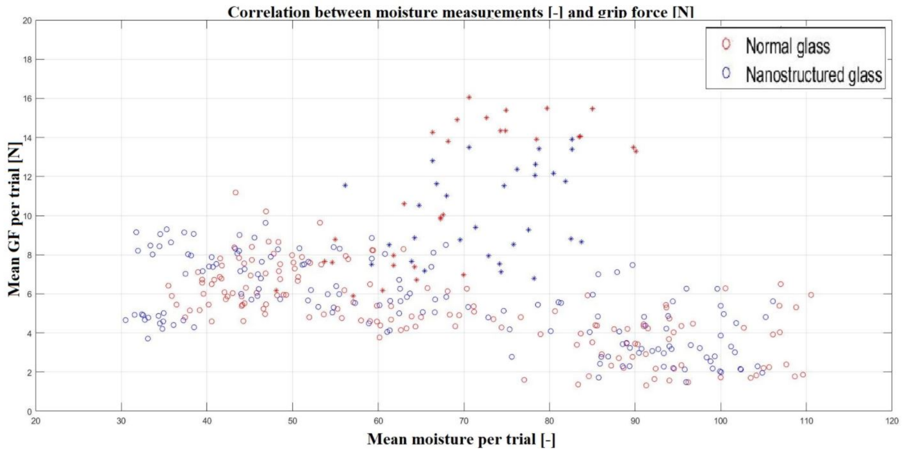

Figure 19: Correlation between moisture measurements and mean grip force [N] across all the subjects. The data of the subject 4 and 10 are marked with asterisks to highlight them. Red lines refer to the normal glass, blue lines refer to the nanostructured glass. Vertical black doted lines delimit the trials.

The influence of the occlusion phenomenon, i.e. the increase in moisture level within each trial, on the grip force, was also investigated by computing a correlation between the variation of moisture within trials and the variation of grip force between the 3 last and the 3 first oscillation of the trials. The result is depicted on Figure 20. No significant correlation was found but a trend was present: obvious decreasing variations in grip force between the beginning and the end of the trials (i.e. negative values in the x-axis on Figure 20) correspond to the highest values of moisture differences. This means that large variation in grip force within a trial often corresponds to a large increase in the moisture level.

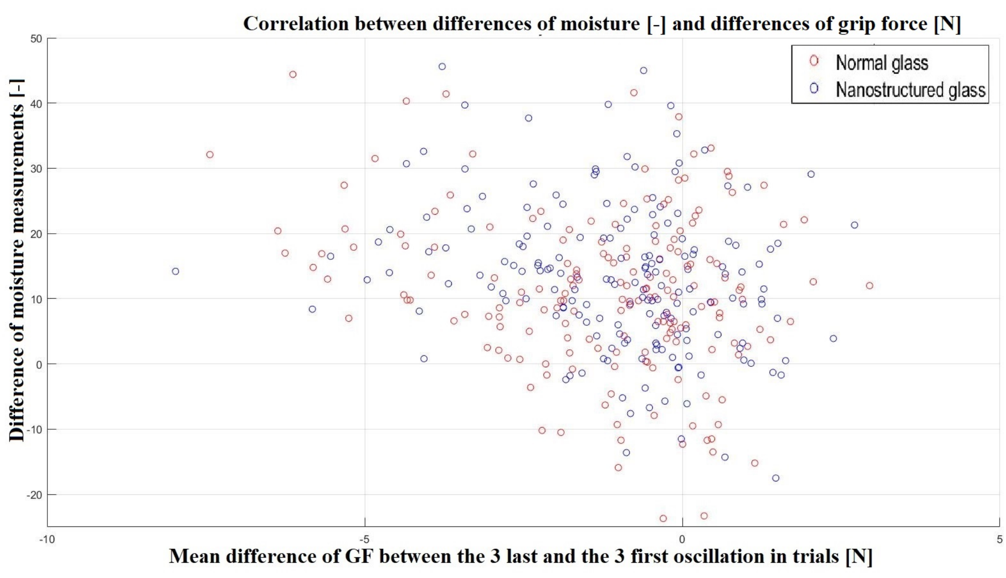

Figure 20: Correlation between differences of moisture [-] and differences of grip force [N]. Red lines refer to the normal glass, blue lines refer to the nanostructured glass. Vertical black doted lines delimit the trials.

3.4.3 Grip force modulation evolution

The grip force modulation was computed as the grip force range during each oscillation, i.e. the difference between its global maximum and global minimum values. It is therefore not a continuous but a discrete signal. The obtained results for the whole practical session of all subjects are depicted on Figure 21.

The analysis of this parameter needs to look at the evolution of the grip force in parallel. Indeed, if a diminution in the grip force modulation is noticed, its interpretation is not the same if the grip force is stable or also decreases.

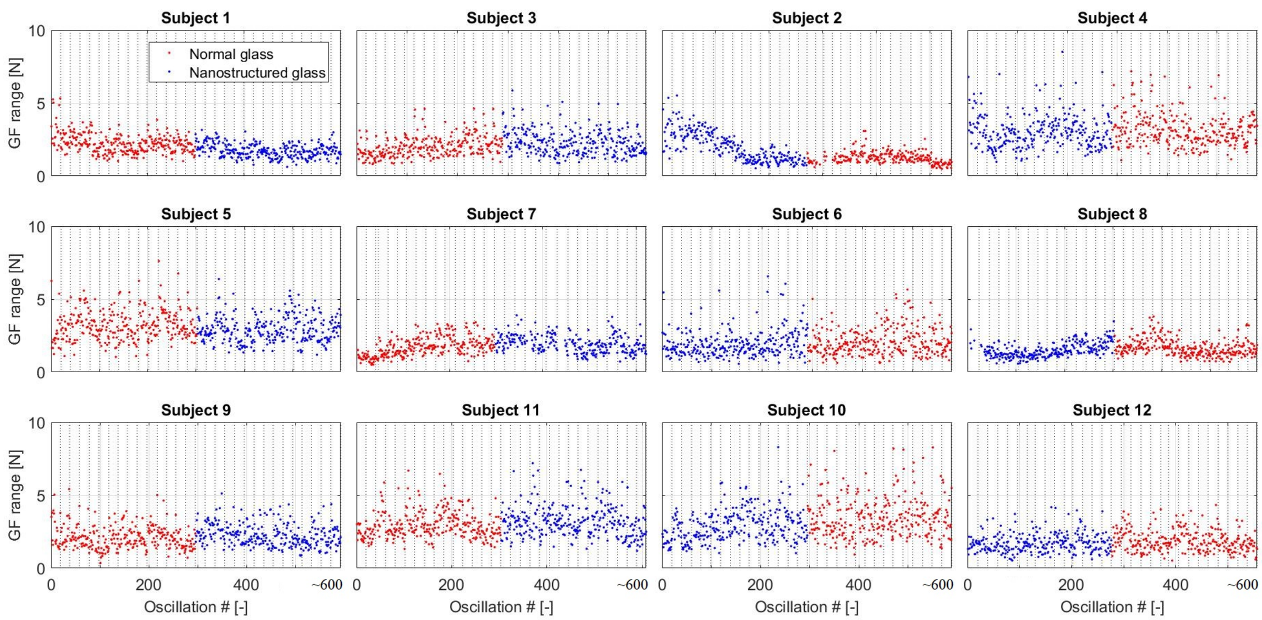

Figure 21: Evolution of the grip force modulation [N] (max GF - min GF) across all the trials of all the subjects. Red lines refer to the normal glass, blue lines refer to the nanostructured glass. Vertical black doted lines delimit the trials.

Different trends can be analysed when looking at Figure 21. It presents data which considerably fluctuates between subjects as well as throughout the experimental session.

In Table 6 are presented the average values of the grip force modulation evaluated for each subject and each type of glass. Slight variations may be observed on their basis, but a more in-depth analysis must be carried out in order to fully understand its evolution.

Subject #	1	2	3	4	5	6	7	8	9	10	11	12
N.G.	2.25	1.25	2.02	3.17	3.23	2.08	1.72	1.67	2.12	3.55	2.96	1.88
NS.G.	1.74	2.00	2.30	3.05	2.92	1.95	1.93	1.52	2.27	2.88	3.20	1.76

Table 6: Means of grip force modulation values [N] for each subject and both types of glass.

The adaptation of the grip force modulation within each trials block depends mostly on the adaptation of the grip force within the trials block. For some subjects, since their mean grip force per trial decreases within the trials blocks, their modulation evolves in the same way. This trend can be observed for each of the subjects for whom a statistical difference between the modulation at the beginning and at the end of a trials block was found (subjects 3, 7 and 9 for the normal glass, and subjects 1, 2, 3, 7, and 11 for the nanostructured glass). The relation between a grip force decrease and a grip force modulation decrease is clearly observable during the trials block of the subject 2 with the nanostructured glass. For both glasses, no statistical difference was observed at the level of the population (p-value$_{N.G} = 0.79$ and p-value$_{NS.G} = 0.22$).

The evolution of the grip force modulation within trials is of bigger interest. A change of grip force modulation within trials shows if the grip force can be rapidly modulated. On Figure 21, a visual clue of this intra-trial modulation is the presence of some isolated points at a high value of range at the beginning of each trial (defined by the vertical dotted black lines). At the individual level, 6 subjects (subjects 1, 3, 4, 5, 7 and 10) present a significant difference in their modulation within trials. This phenomenon is also observable in the case of the nanostructured glass, for which 7 subjects (subjects 1, 3, 5, 7, 8, 9 and 10) have a statistical change in their grip force modulation. This trend is confirmed by statistics realised on the population, for each of the 2 glasses (p-value$_{N.G}$= 0.02 and p-value$_{NS.G.}$= 0.04).

Comparison between both types of glass

At the level of the population, no statistical difference was observed between the averaged grip force modulation on the 2 types of glass (p-value = 0.77).

The grip force modulation was found to be statistically different between both glasses for 3 subjects, either for the evolution within trials blocks (subjects 2, 3 and 7) or for the evolution within trials (subjects 3, 9 and 10). However, the statistics on the population did not confirm these trends, with a p-value of 0.21 and a p-value of 0.42 respectively.

Influence of the moisture level on the grip force modulation

To analyse the influence of the moisture on the grip force modulation, the same correlations than the ones performed to investigate the impact of the moisture on the grip force were computed. However, no correlation nor clear tendency were observed.

3.4.4 Safety margin evolution

Another way to investigate the evolution of the subjects' behaviour during the manipulations is to look at the safety margin they maintained. The safety margin is defined as the difference between the grip force applied by the subject and the grip force slip, which is the minimum grip force to be applied to prevent the object from slipping. The latter depending on the coefficient of friction, it is therefore also the case for the safety margin. The evolution of this variable maintained by each subject throughout the experimental session is depicted on Figure 22.

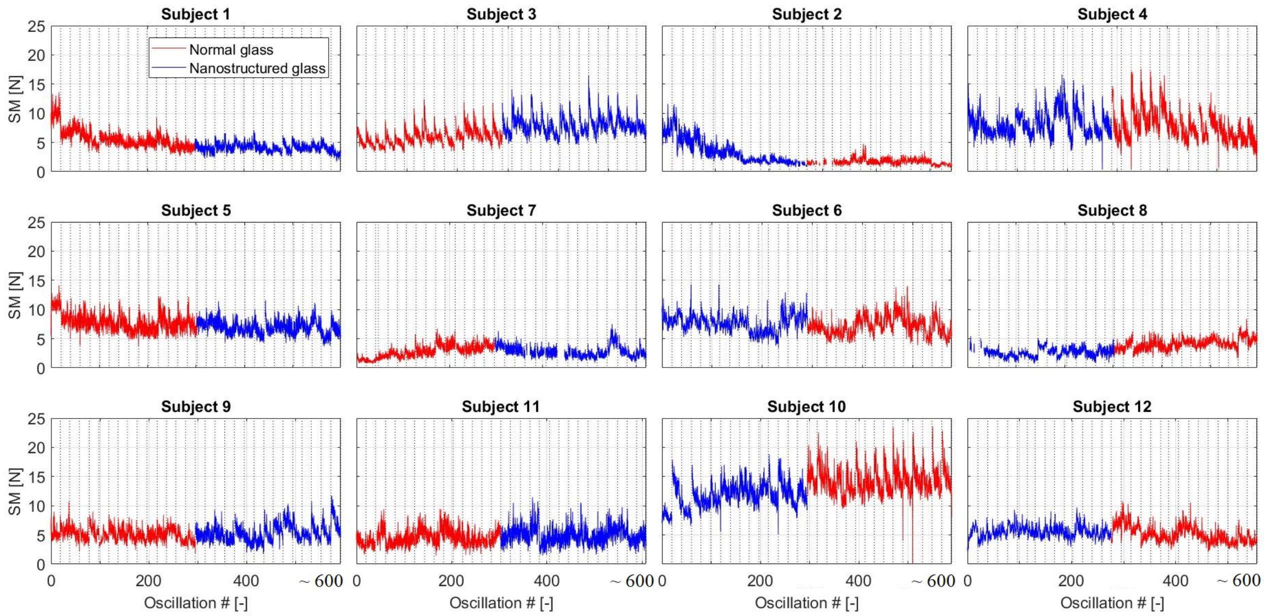

Figure 22: Evolution of the safety margin [N] (GF - Slip F) across all the trials of all the subjects. Red lines refer to the normal glass, blue lines refer to the nanostructured glass. Vertical black doted lines delimit the trials.

Even if Figure 22 looks similar to Figure 18, it is not. This illusion is due to the fact that the slip forces computed using the coefficients of friction previously presented are of small amplitude, as reflected by their mean values per trials blocks, which are available in Table 7. The amplitude of the safety margin is therefore close to but not equal to the grip force, especially since like the grip force, the slip force varies during manipulations.

Subject #	1	2	3	4	5	6	7	8	9	10	11	12
N.G.	0.30	0.23	0.31	0.30	0.27	0.11	0.24	0.17	0.18	0.28	0.42	0.21
NS.G.	0.47	0.26	0.53	0.34	0.54	0.16	0.20	0.28	0.14	0.27	0.42	0.25

Table 7: Means of slip force values [N] for each subject and both types of glass.

Within the trials blocks or within the trials, exactly the same trends were observed for the safety margin than the ones previously exposed about the grip force (there is no statistical difference between safety margin within each trials block but one within the trials for each glass). This means that no matter how much the slip force varies during the manipulations, it is not sufficient to have a significant impact on the safety margin applied by the subjects.

Comparison between both types of glass

Once again, no difference with the detected trends on the grip force was found by looking at the evolution of the safety margin between both glasses.

3.5 Finger pad deformations

3.5.1 Center of pressure position evolution

As a remainder, the center of pressure is the point were the resultant force is applied by the subject on the object. Even if the information about it is not part of the fingertips images recorded during manipulations, it can provide information about the finger pad deformations. Indeed if the center of pressure moves during manipulations, that means that some deformations are occurring at the contact area between the fingertip and the object. It is due to the visco-elasticity of the fingerpad, which therefore deforms under tangential loading. This displacement is a good estimation of the rolling appearing during oscillation movements: when deforming, parts of the fingerpad, which were or were not part of the initial contact area between the fingerpad and the object loses or gains contact with the surface. This phenomenon is a peeling mechanism, and is not due to a tissue change.
On Figure 23 and Figure 24 are shown the means of the COP displacement of each of the 2 fingers for both glasses and subjects.

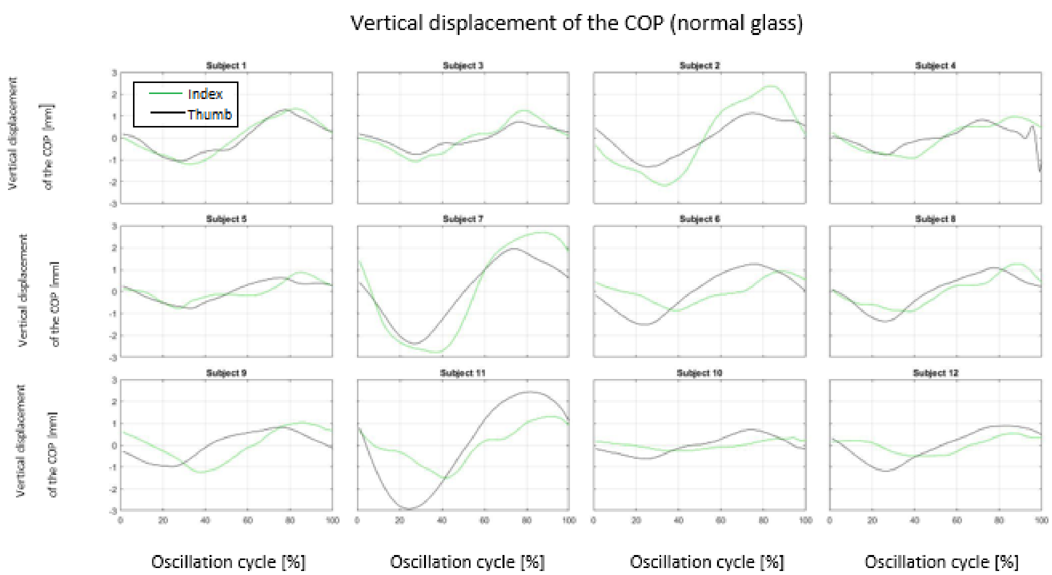

Figure 23: COP displacement [mm] along an oscillation cycle, for both fingers of all subjects for the normal glass. The green line represents the displacement of the index COP, whereas the black line represents the displacement of the thumb COP.

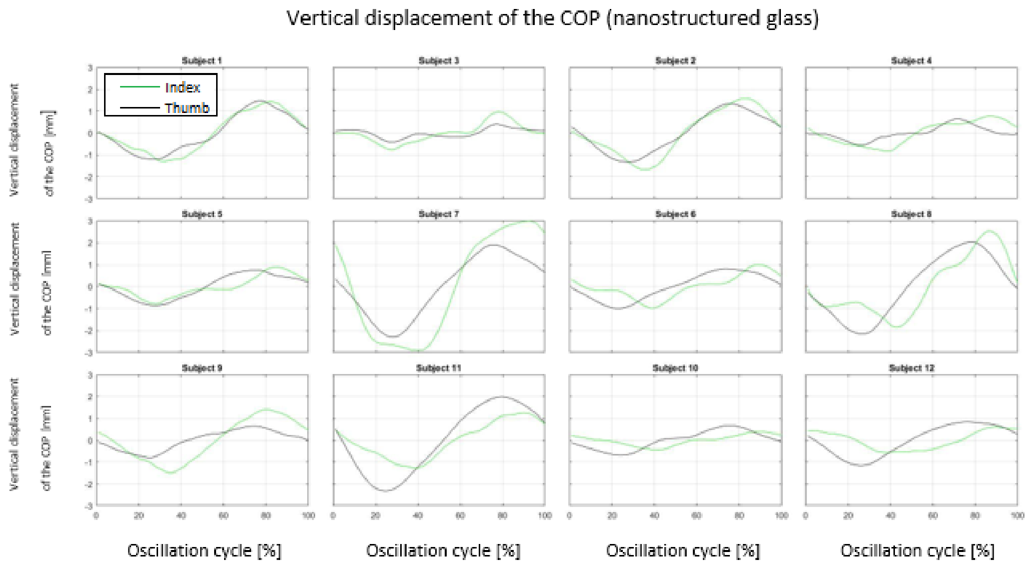

Figure 24: COP displacement [mm] along an oscillation cycle, for both fingers of all subjects for the nanostructured glass. The green line represents the displacement of the index COP, whereas the black line represents the displacement of the thumb COP.

It can be seen on these figures that COP displacement varies around its initial position along the oscillation cycle. When the manipulandum is at the higher value of the oscillation, the COP tends to move downwards. On the contrary, when the manipulandum reached its minimal position value, the COP moves upwards.

For the same glass condition, the displacement of the COP of the two fingers of the subjects can be either really close (see subject 1 with the nanostructured glass) or presenting some variations between them (see subject 11 with the normal glass).

Moreover, the COP displacement can vary from subject to subject. Example given, whereas subject 10 presents very small COP displacement, subjects 7 or 11 impress with their center of pressure displacement. The maximum values of this displacement all subjects combined approaches the 3 mm upwards and downwards.

When comparing both types of glass, some fluctuations exist but the subjects kept the same order of magnitude of movement (subject 7 moved a lot with both glasses, while subject 12 moved little with both glasses).

3.5.2 Slips detection

So as to understand what was the strategy of the subjects during the manipulations, it is interesting to know if they let some sliding appeared. In order to find it out, as explained in Section 2, the vertical displacement of the feature point that moved the least between the first and the last frames was computed by oscillation. The results for all subjects throughout the entire experimental session are represented in Figure 25. It is important to note that for reasons of visibility not all subfigures have the same scale.

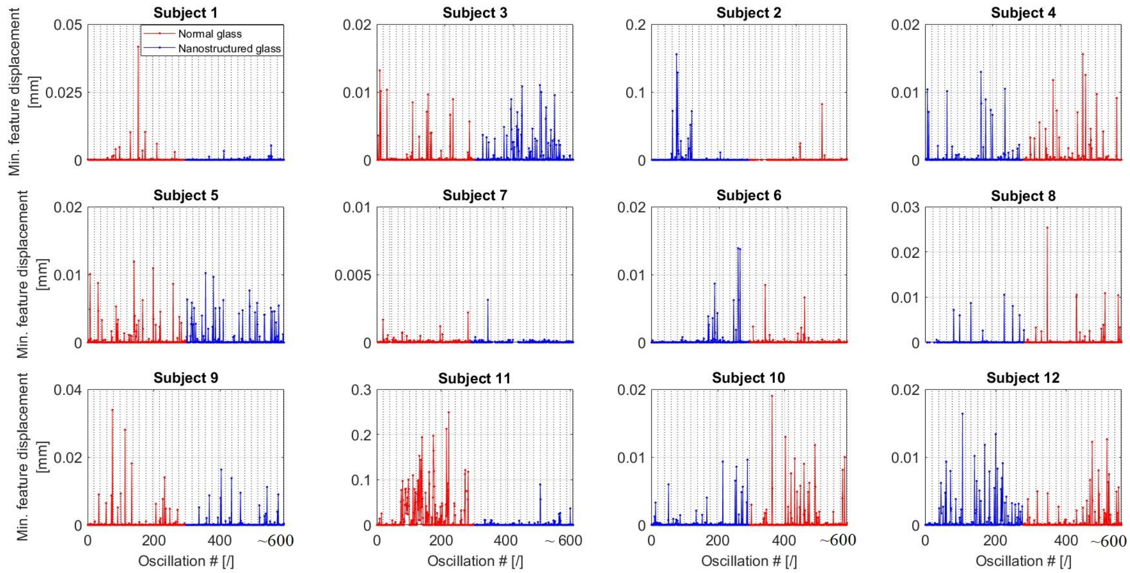

Figure 25: Minimal displacement [mm] of the feature point that moved the least between the first and last frame of each oscillations. Red lines refer to the normal glass, blue lines refer to the nanostructured glass. Vertical black doted lines delimit the trials.

Considering that a point has slipped if it has travelled a distance of more than one pixel ($\approx$ 0.016 mm), only a few subjects show slippage with certainty: subject 2 using nanostructured glass as well as subject 16 using normal glass. It is also possible to consider subjects 1, 8 and 9 as having slipped using normal glass but with some hesitation.

With so few conclusive results, it is therefore difficult to draw conclusions, not only on the evolution of displacements within trials blocks and within trials, but also to compare them between the 2 types of glass. The only interesting remark that can be made is that the 2 subjects for whom it is clear that the slipping has occured are the 2 subjects for whom a wet skin was detected. Once again, it tends to prove that the moisture content of the fingertip skin plays a key role in maintaining a stable precision grip.

3.5.3 Surface strain rates analysis

When the fingerpad is subject to both normal and tangential loading, surface strains developed at its surface, in the form of compression, relaxation and shear stress. By looking at the evolution of the strain during one oscillation cycle, it can be seen that a recurrent and reproducible pattern occurs. To visualise them, Figure 26 can be observed. This figure was taken from a previous work [21], and represents the strain rates at different moments during an oscillation cycle. On this figure, the oscillation cycle started with a downward movement, which is not the way the oscillations in this study were segmented. Therefore, the pattern that concerned the 12 subjects that have been tested in the present study is not the same as the one presented here but this latter can be quite easily derived from this figure.

The reproducible pattern occurs at the level of the vertical axial strain when the manipulandum reached its extreme position values. This pattern is a direct consequence of the visco-elastic property of the finger pad. To be more precise, at the upper end of the oscillatory movement, a compression (epsilon$_{yy}$ < 0) in the upper part of the finger and a stretch in the lower part (epsilon$_y y$>0) are deformations of this viscoelastic body caused by its negative acceleration and especially by the transmission of a downward force from this viscoelastic body to the object in order to slow down its ascent and finally make it descend.

The extreme vertical position of the manipulandum led therefore to the strain principal components to reach their maximal values.

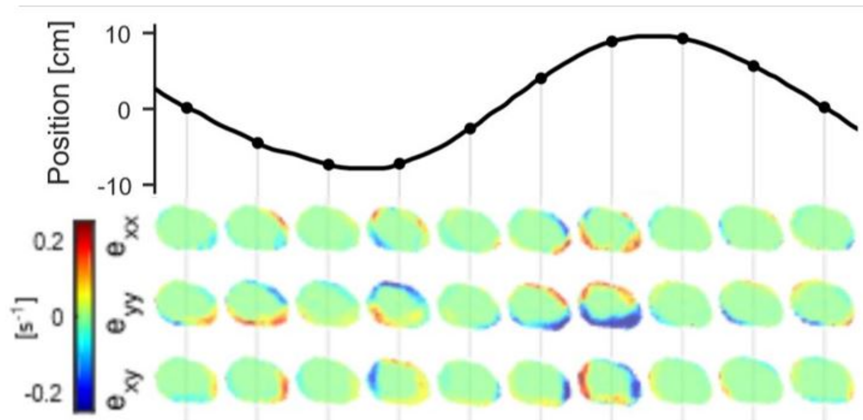

Figure 26: Strains appearing at the surface of the finger pad depending on the position of the manipulandum in the oscillation cycle. [21]

.

4 Conclusion

At the end of this study, I did not reach the primary objective of this master thesis: to compare the force adaptation occurring when manipulating 2 objects with different frictions on the basis of forces and fingerprints images analyses.

At the level of the force analysis, no clear and significant population trend could be drawn regarding the impact of a change in friction. A large variability in subject behaviours was observed.

In terms of the image analysis, convincing results were unfortunately insufficient to link them with the force analysis. Although the analysis of the images made it possible to approximate the deformations suffered by the finger pad during oscillation cycles, it was not possible to explain the mechanism at the level of forces.

Finally, the only significant influence noted at most stages of the analysis was the humidity level. In terms of the coefficient of friction, as well as grip force or slips, subjects with different skin moisture content tended to behave differently. Literature has proven that skin moisture greatly influences force control during manipulations in precision grip. For an optimal moisture content, an influence on both the forces and the mechanical properties of the finger pad is observed. This study tends to confirm this both in terms of force adaptation and image analysis.

5 References

[1] Johansson, Roland S.; Flanagan, J. Randall. *Coding and use of tactile signals from the fingertips in object manipulation tasks.* In: *Nature Reviews Neuroscience*, Vol. 10, p. 345-359 (2009)

[2] Johansson, Roland S.; Vallbo, Ake B. *Tactile sensory coding in the glabrous skin of the human hand.* In: *Trends in Neurosciences*, Vol. 6, p. 27-32 (1983)
[3] Barrea, Allan. *Finger pad mechanics, tactile signals and dexterous manipulation.* Prom. : Thonnard, Jean-Louis ; Lefèvre, Philippe

[4] MitsuoKawato. *Internal models for motor control and trajectory planning.* In: *Current opinion in neurobiology*, Vol. 6, (1999)

[5] Westling, Göran; Johansson, Roland. *Factors influencing the force control during precision grip.* In: *Experimental brain research. Experimentelle Hirnforschung. Expérimentation cérébrale* , Vol. 53, p. 277-84 (1984)

[6] Johnson, Kenneth. *The roles and functions of cutaneous mechanoreceptors.* In: *Current Opinion in Neurobiology* , Vol. 11, no.4, p. 455-61 (2001)

[7] Augurelle, Anne-Sophie; Smith, Allan ; Lejeune, Thierry ; Thonnard, Jean-Louis. *Importance of cutaneous feedback in maintaining a secure grip during manipulation of hand-held objects.* In: *Journal of Neurophysiology* , Vol. 89, no.2, p. 665-71 (2003)

[8] Witney, Alice; Wing, Alan; Thonnard, Jean-Louis; Smith, Allan. *The cutaneous contribution to adaptive precision grip.* In: *Trends in neurosciences* , Vol. 27, no.10, p. 637-43 (2004)

[9] Andre, Thibaut; Lévesque, Vincent; Hayward, Vincent ; Lefèvre, Philippe ; Thonnard, Jean-Louis. *Effect of skin hydration on the dynamics of fingertip gripping contact.* In: *Journal of the Royal Society Interface* , Vol. 8, no.64, p. 1574-83 (2011)

[10] Delhaye, Benoit; Lefèvre, Philippe; Thonnard, Jean-Louis. *Dynamics of fingertip contact during the onset of tangential slip.* In: *Journal of the Royal Society Interface* , Vol. 11, no.100, p. 1-11 (2014)

[11] Delhaye, Benoit; Barrea, Allan; Edin, Benoni; Lefèvre, Philippe ; Thonnard, Jean-Louis. *Surface strain measurements of fingertip skin under shearing.* In: *Journal of The Royal Society Interface* , Vol. 13, no.115, p. 1-11 (2016)

[12] Barrea, Allan; Delhaye, Benoit P.; Lefèvre, Philippe; Thonnard, Jean-Louis. *Perception of partial slips under tangential loading of the fingertip.* In: *Scientific Reports*, Vol. 8, 7032 (2018)

[13] Inamoto M.; Tomeno S. *Control Tactile Feel of Glass by Visually Imperceptible Structure* 2019 IEEE World Haptics Conference (WHC), (2019)

[14] *Corneometer® CM 825: Measurement Principle*, Courage + Khazaka electronic GmbH, Accessed on the 4^{th} of July.

[15] Barrea, Allan; Cordova Bulens, David; Lefèvre, Philippe ; Thonnard, Jean-Louis. *Simple and reliable method to estimate the fingertip static coefficient of friction in precision grip.* In: *IEEE Transactions on Haptics* , Vol. 9, no.4, p. 492-498 (2016)

[16] André, Thibaut; Lefèvre, Philippe; Thonnard, Jean-Louis. *A continuous measure of fingertip friction during precision grip.* In: *Journal of neuroscience methods*, Vol. 179, no.2, p. 224-9 (2009)

[17] André, Thibaut ; Lefèvre, Philippe ; Thonnard, Jean-Louis. *Fingertip Moisture Is Optimally Modulated During Object Manipulation.* In: *Journal of Neurophysiology* , Vol. 103, no.1, p. 402-8 (2010)

[18] André, Thibaut ; Lefèvre, Philippe ; Thonnard, Jean-Louis. *Fingertip Moisture Is Optimally Modulated During Object Manipulation.* In: *Journal of Neurophysiology* , Vol. 103, no.1, p. 402-8 (2010)

[19] Augurelle, Anne-Sophie; Penta, Massimo; White, Olivier ; Thonnard, Jean-Louis. *The effects of a change in gravity on the dynamics of prehension.* In: *Experimental brain research. Experimentelle Hirnforschung. Expérimentation cérébrale* , Vol. 148, no.4, p. 533-40 (2003)

[20] Bleyenheuft, Yannick; Lefèvre, Philippe ; Thonnard, Jean-Louis. *Predictive Mechanisms Control Grip Force After Impact in Self-Triggered Perturbations.* In: *Journal of motor behavior*, Vol. 41, no.5, p. 411-7 (2009)

[21] Delhaye, Benoit; Schiltz, Félicien; Thonnard, Jean-Louis; Lefèvre, Philippe. *Imaging the fingerpad deformations during vertical oscillations of a hand-held object*

UNIVERSITÉ CATHOLIQUE DE LOUVAIN
École polytechnique de Louvain
Rue Archimède, 1 bte L6.11.01, 1348 Louvain-la-Neuve, Belgique | **www.uclouvain.be/epl**